Title	Piezoelectric properties of aligned collagen membranes
Authors(s)	Denning, Denise; Paukshto, M. V.; Habelitz, S.; Rodriguez, Brian J.
Publication date	2014-02
Publication information	Journal of Biomedical Materials Research Part B: Applied Biomaterials, 102 (2): 284-292
Publisher	Wiley
Item record/more information	http://hdl.handle.net/10197/5139
Publisher's statement	This is the author's version of the following article: TDenning D., Paukshto M. V., Habelitz S., Rodriguez B. J.. 2013. Piezoelectric properties of aligned collagen membranes. J þÿ B i o m e d M a t e r R e s P a r t B 2 0 1 3 : 0 0 B : 0 0 0 0 0 0 w h i c h h a s b e e http://dx.doi.org/10.1002/jbm.b.33006
Publisher's version (DOI)	10.1002/jbm.b.33006

Piezoelectric properties of aligned collagen membranes

D. Denning,[1,2] M. V. Paukshto,[3] S. Habelitz,[4] and B. J. Rodriguez[1,2,*]

[1]Conway Institute of Biomolecular and Biomedical Research, University College Dublin, Belfield, Dublin 4, Ireland.

[2]School of Physics, University College Dublin, Belfield, Dublin 4, Ireland.

[3]Fibralign Corporation, 1230 Bordeaux Drive, Sunnyvale, CA 94089, USA.

[4]Department of Preventive and Restorative Dental Sciences, University of California, 707 Parnassus Ave., San Francisco, CA 94143-0758, USA.

Abstract

Electromechanical coupling, a phenomenon present in collagenous materials, may influence cell-extracellular matrix interactions. Here, electromechanical coupling has been investigated via piezoresponse force microscopy in transparent and opaque collagen membranes consisting of helical-like arrays of aligned type I collagen fibrils self-assembled from acidic collagen solution. Using atomic force microscopy, the transparent membrane was determined to contain fibrils having an average diameter of 76 ± 14 nm, while the opaque membrane comprised fibrils with an average diameter of 391 ± 99 nm. As the acidity of the membranes must be neutralized before they can serve as cell culture substrates, the structure and piezoelectric properties of the membranes were measured under ambient conditions before and after the neutralization process. A crimp structure (1.59 ± 0.37 μm in width) perpendicular to the fibril alignment became apparent in the transparent when the pH was adjusted from acidic (pH = 2.5) to neutral (pH = 7) conditions. In addition, a 1.35 fold increase was observed in the amplitude of the shear piezoelectricity of the transparent membrane. The structure and piezoelectric properties of the opaque membrane were not significantly affected by the neutralization process. The results highlight the presence of an additional translational order in the transparent membrane in the direction perpendicular to the fibril alignment. The piezoelectric response of both membrane types was found to be an order of magnitude lower than that of collagen fibrils in rat tail tendon. This reduced response is attributed to less-ordered molecular assembly than is present in D-periodic collagen fibrils, as evidenced by the absence of D-periodicity in the membranes.

*corresponding author: brian.rodriguez@ucd.ie

I. Introduction

The origin and the biofunctional implications of piezoelectricity in collagen fibrils have been topics of debate since the discovery of piezoelectricity in bone in 1957 [1]. Type I collagen is the most abundant protein in mammals, and the complex hierarchical structures of various collagenous tissues contribute to a variety of functions, e.g., load-bearing tendon and transparent cornea [2]. In addition to the outstanding tensile strength of collagen fibrils [3], cellular interactions with collagen fibrils in the extracellular matrix are believed to play a fundamental role in cell proliferation, cell signaling, cell attachment, and tissue restructuring [4-7]. The origin of the unique mechanical and electromechanical properties of collagenous tissues, however, remains largely unknown [8]. It is only recently that researchers are beginning to understand the mechanism for force transmission between collagen molecules within fibrils on the nanoscale [9]. The need for understanding the structural and functional roles of collagenous materials is of vital importance for tissue engineering applications. Recently, it was shown that glucose suppresses ferroelectricity in aortic elastin [10], which highlights the importance of understanding the biofunctional role of physical and electrical properties such as piezoelectricity in biomaterials. Previous studies have shown that collagen assembly is greatly affected by pH and also by the presence of electrolytes (e.g., KOH [11]), but the effects of such parameters on the functional properties, including piezoelectricity, of collagen fibrils has yet to be fully investigated.

Piezoelectricity is the linear coupling between a mechanical stimulus and an electrical response. Since the discovery of piezoelectricity in bone by Fukada and Yasuda [1], there have been significant efforts made toward understanding the possible role piezoelectricity plays in Wolff's law (whereby bone adapts to an applied stress) [12]. Piezoelectricity was also observed in tendon by Fukada and Yasuda [13], but with a ~14 fold increase in magnitude (d_{14} coefficient) compared to bone, suggesting that collagen is responsible for piezoelectricity in bone. Another study, which involved the demineralization and decollagenation of bone, determined conclusively that the primary mechanism of piezoelectricity in bone is collagen piezoelectricity [14]. This piezoelectricity is thought to result from the quasi-hexagonal packing of collagen molecules (symmetry group, C_6) in the fibril cross section, which leads to a predominantly shear piezoelectricity in the axial direction [1, 15]. Piezoresponse force microscopy (PFM) is an adaptation of atomic force microscopy (AFM) which detects bias-induced surface deformations

via the converse piezoelectric effect. This technique enables investigations of electromechanical coupling in biosystems at the nanoscale [16], and potentially in physiologically relevant environments [17-19]. PFM has contributed considerably in the investigation of electromechanical coupling in biosystems, including collagen and bone [20-22]. While mechanical and structural properties are studied extensively for tissue engineering applications (collagenous scaffolds, hydrogels, etc. [23]), electromechanical coupling has not been addressed as a functional property for these applications until recently [24]. Ferroelectricity has also recently been discovered in aortic tissue [25] and glycine crystals [26], highlighting both the prevalence of electromechanical coupling in biosystems and the lack of current understanding of possible biofunctional implications. Furthermore, practical applications of biopiezoelectricity, e.g., energy harvesting, have been demonstrated [27].

Electromechanical coupling in collagen may be a factor involved in bone remodeling and other biological processes [12]. This necessitates understanding electromechanical coupling in collagen under biologically relevant conditions. To date, only D-periodic collagen fibrils have been investigated for their piezoelectric properties [21, 22, 24]. One previous study reported piezoelectric response from non-fibrillar collagen [28], but the effect of fibrillar structure on piezoelectricity is unknown. Since these collagen membranes are used in neutralized form to investigate cell behavior [29], it is necessary to study the effect of pH on piezoelectric properties of the membranes as well. Here, PFM is used to study the electromechanical properties of collagen membranes with different structures comprising aligned fibrils both before and after a neutralization process, which alters the pH from acidic to neutral conditions.

II. Materials and methods

Two types of collagen samples (Nanoweave, Fibralign) were prepared using a process based on technology developed for liquid crystal display manufacturing [30-33] in which purified molecular collagen solution in the liquid crystal phase [34] was sheared onto glass slides [35]. This method provides control over the diameter, structure, and alignment of the fibrils. One type of sample comprised aligned collagen fibrils with diameters of several hundred nm in a braided matrix, which was optically opaque (henceforth denoted *opaque*). The second type of sample comprised aligned nanofibrils (i.e., having diameters of < 100 nm) and was optically transparent (henceforth denoted *transparent*). Differences in fibril diameter and morphology of the collagen

membranes were obtained during the preparation by changing the osmolality of the initial molecular collagen solution. The *transparent* membrane corresponds to a lower ionic strength than the *opaque* membrane (20 and 80 mOsm/Kg H_2O, respectively). Initially, the aligned collagen samples were in acidic form (pH of 2.5), therefore a simple neutralization process was implemented, which includes incubation in Dulbecco's phosphate buffered saline (pH of 7) for 5 min and rinsing in deionized water to bring the pH of the membrane up to physiological conditions (pH of 7). Directly after the neutralization process, the samples were gently dried with nitrogen and subsequently imaged using AFM. By comparing the weight of similar samples before and after heating to 90 °C in vacuum, it was determined that air dried membranes have a water content of between 15-20%.

Topographical studies of the alignment and structure of the fibrils were performed using a commercial AFM system (MFP-3D, Asylum Research) in both amplitude modulation and contact mode. During PFM experiments, a 5 kHz AC voltage of 30 V (peak-to-peak) was applied to a conductive cantilever probe (DPE18, Mikromasch), which resulted in local surface deformations via the converse piezoelectric effect. The nominal spring constant and resonant frequency of the cantilevers used were 3.5 Nm^{-1} and 75 kHz, respectively. These surface oscillations at the excitation frequency were demodulated into amplitude and phase (related to the amplitude of deformation and polar orientation, respectively) using an external lock-in amplifier (HF2LI, Zurich Instruments). Calibration of the vertical sensitivity (via force curve) of the cantilever was performed before and after the experiment (difference of 1%). Lateral calibration of the cantilever was undertaken based on the geometry of the lever used [36]. The ratio (R) of the in-plane to out-of plane amplification is given by $R = 2L/3h$, where L is the length of the cantilever used and h is the combined height of the tip and the thickness of the cantilever (nominally 230 μm and 18 μm, respectively). High voltage PFM imaging was implemented via a custom built high voltage system based on a PA85 amplifier, which allowed for a 10-fold amplification of the excitation AC signal. PFM amplitude images were normalized to the image with the largest piezoresponse for each membrane type (leading to a scaling factor of 10) in order to directly compare the PFM signal between samples before and after the neutralization process.

III. Results and Discussion

AFM analysis of collagen structure

AFM has been used in order to distinguish topographical differences between the *transparent* and *opaque* collagen membranes. Fig. 1 displays amplitude modulation AFM images obtained for both membranes. An AFM height image of the *transparent* membrane is shown in Fig. 1a. The white arrow in Fig. 1a represents the direction of fibrillar alignment. The fibrils have small and relatively uniform fibrillar widths (75.9 ± 14.3 nm; n = 20). However, it is possible that the tip radius exceeds the width of the nanofibrils, which would lead to tip broadening. Collagen fibrils assembled in ideal physiological conditions *in vitro*, or indeed collagen fibrils produced *in vivo*, give rise to a staggered alignment of collagen molecules resulting in gap zones. This leads to the well-known D-periodicity (~ 67 nm) associated with type I collagen fibrils [8]. AFM height and amplitude images of a 1 × 1 μm^2 area (Fig. 1b and 1c, respectively) reveal additional surface details showing that the nanofibrils have a non-periodic structure. The AFM height image of the *opaque* membrane displayed in Fig. 1d, has a different structure to that seen for the *transparent* membrane. The fibrillar widths are ~ 5 times larger (391.1 ± 98.7 nm) than those observed in the *transparent* membrane. There is no apparent periodicity associated with the fibrils of the *opaque* membrane (from the AFM amplitude image, Fig. 1e), indicating they are non D-periodic type I collagen fibrils. AFM height and amplitude images of a 5 × 5 μm^2 area (Fig. 1e and 1f, respectively) confirm the absence of D-periodicity in the *opaque* membrane.

In comparison with known tissues, the fibrillar widths of the transparent cornea are 20-50 nm [37, 38], which is the same order of magnitude as the fibrils in the *transparent* membrane. In addition, the fibrils in the *transparent* membrane are oriented, a feature shared by corneal lamellae. Moreover, corneal fibroblasts plated on the *transparent* membrane have been found to express a normal quiescent phenotype, further highlighting the similarities between the *transparent* membrane and cornea [39]. The range of widths in the *opaque* membrane is in the range found in opaque tendon, which is between 20 - 500 nm [40]. The uniform width and structure of the fibrils in both membranes highlights to an extent the range of structures that can be made using the liquid crystal approach.

PFM analysis of electromechanical properties of collagen membranes – before and after neutralization

A collagen fibril is a shear piezoelectric [22, 23]. Therefore, only lateral PFM (LPFM) has been employed for this investigation. AFM and PFM images of the *transparent* membrane before

neutralization are shown in Fig. 2. Fig. 2a is an AFM height image of a 15 × 15 μm^2 scan area obtained in contact mode. There is a predominant alignment of the nanofibrils, which is indicated via the white arrow in Fig. 2a. The piezoelectric properties of the *transparent* membrane are visualized in Fig 2b. The nanofibrils are organized into large piezoelectric 'domains' whereby a domain is defined as an area of uniform polarization. The averaged piezoresponse value over 10 randomly selected domains was calculated from Fig. 2b to be 0.467 ± 0.105 a.u. The piezoresponse of each domain was calculated via image processing using 1 × 1 μm^2 square masks (Igor Pro, Wavemetrics), which allowed the piezoresponse over this predefined area to be averaged. The LPFM images confirm that the shear piezoelectric properties of type I collagen fibrils is replicated in these *transparent* membranes. The average size of the domains is 1.65 ± 0.92 μm, indicating there are ~ 20 nanofibrils in each domain. The size of these domains is 1-2 orders of magnitude larger than those seen in either tendon or eye tissues (the domains are sized between 70–400 nm) [40]. The domains take on the structure of the membrane, possibly a result of the induced structural orientation of the nanofibrils, but the domains do not correlate directly with the topography. The LPFM phase image, shown in Fig. 2c, reveals the polarity of each domain. This is related to the orientation of the dipole in collagen molecules (from amine (N) to carboxyl (C) termini). The 180° phase shift between neighboring domains demonstrates that the direction of the N to C polarity of the two domains is opposite. Analysis of the LPFM amplitude image of a 5 × 5 μm^2 area (Fig. 2e) shows there is a ~ 0.25 fold difference between the piezoresponse amplitude of opposing domains. As oppositely oriented domains are expected to exhibit the same amplitude response, this variation could be related to the tip-sample capacitance and to the choice of imaging frequency [41]. Inspection of the AFM height image and the corresponding PFM phase image reveals that the phase contrast inverts for some fibrils when their orientation changes with respect to the cantilever axis. This polarity reversal of bent collagen fibrils with respect to the cantilever-fibril orientation has been demonstrated previously [42] and illustrates the orientation dependence of PFM [39]. An example is highlighted with black and white arrows in Fig. 2 (d-f).

After the neutralization process, the pH is adjusted to physiological conditions (pH 7). Fig 3 displays the AFM and PFM results for the *transparent* membrane after neutralization. The topography over a 15 × 15 μm^2 scan area (Fig. 3a) is different to that seen before the neutralization process. The fibrils have a similar alignment, however, a crimped structure [43]

also appears, which is generally perpendicular to the direction of fibrillar alignment. The average width of the crimped structure is 1.59 ± 0.37 μm (n = 10), which is one order of magnitude smaller than that seen in natural tendon tissue (10 – 100 μm) [43]. Interestingly, the crimped structures have the same statistical width as the piezoelectric domains (1.65 ± 0.92 μm). It is possible that there exists a correlation between the size of the crimped structure and the domain size, but verification would require additional investigation. The lateral piezoresponse also changes significantly. The shape and width of the piezoelectric domains (Fig. 3b) remain statistically the same, but there is a 1.5 fold increase (0.703 ± 0.058 a.u.; n = 10) in the amplitude of the lateral piezoresponse. When averaging only the domains from Fig. 2e, which have a larger response in the before neutralization image (0.524 ± 0.034 a.u.), the increase in piezoresponse compared to the domains from the after neutralization image (Fig. 3e) is still statistically significant (1.35 fold). It is possible that this increase in shear piezoelectricity is due to the neutralization process. As the pH of a protein deviates from neutral conditions, the structure of the protein changes. Thus, the functional activity of the protein can drastically decrease [46]. PFM imaging was performed directly after drying the sample. The measurement was repeated on a second *transparent* membrane, which confirmed the increase (1.2 fold in this instance) in piezoelectric signal after neutralization (data not shown). Hence, based on these measurements, the magnitude of the shear piezoelectric response increases on average 1.35 fold in the *transparent* membrane after adjustment from acidic to physiological pH. The second measurement was carried out over the course of two hours in order to exclude any changes in the observed piezoelectric signal due to changes in of the moisture content of the sample following the neutralization process. The measured piezoelectric signal did not change during this time. The calibration of the cantilever was performed before and after each experiment, which revealed there was a maximum of a 1.01 fold increase in signal due to a change in the properties of the tip. The calibration via force curve was also repeated (n = 10) in order to determine the error in calibration, which was 1.03 fold. These measurement errors are all outside the increase in signal, which proves the observed increase was not due to a change in the properties of the tip. The LPFM phase image (Fig. 3c) displays the N to C polarity of piezoelectric domains of collagen after adjustment to a physiological pH. An AFM height image of a 5 × 5 μm^2 area (Fig. 3d) highlights the appearance of a crimp structure in the collagen matrix. The crimps are indicated via dashed white lines. The LPFM amplitude image (Fig. 3e) of the same area shows

the familiar domain pattern and 1.5 fold increase in piezoelectric response compared to that seen before neutralization in Fig. 2e.

The same measurements were also performed on the *opaque* collagen membrane. Over a 15×15 μm^2 scan area (Fig. 4a), before neutralization, it is again clear that the collagen fibrils in the *opaque* membrane have a larger fibrillar width to that of the *transparent* membrane from the AFM height image. Shear piezoelectricity is confirmed in the *opaque* membrane as seen from the LPFM amplitude image in Fig. 4b. The non D-periodic fibrils in the *opaque* membrane also organize themselves into domains where the piezoelectric domains have an average width of 0.390 ± 0.098 μm. The structure of the domains is somewhat similar to the *transparent* membrane, consisting of domains aligned in the direction of fibrillar orientation. The *opaque* membrane, however, has a smaller average domain width. The average piezoresponse of 10 domains is 0.605 ± 0.037 a.u., which is larger (before neutralization) than the *transparent* membrane. The confirmation here that non D-periodic type I collagen fibrils also exhibit shear piezoelectricity is an interesting result given the origin of piezoelectricity in collagen fibrils is attributed to the hexagonal packing of monomers, which is only present in D-periodic fibrils [1]. It has been postulated that the presence of the D-periodicity in type I collagen fibrils is due to the lateral interaction between collagen molecules [44], and the absence of D-periodicity arises when the lateral assembly of the molecules is distorted. This, combined with our results, would imply that piezoelectricity in type I collagen fibrils does not arise solely from the hexagonal packing of collagen molecules. Our results are consistent with previous studies showing non-fibrillar collagen is piezoelectric [28] and more recently that one of the amino acids present in collagen, namely, glycine, is piezoelectric [26]. The measured shear piezoresponse of the non D-periodic, aligned type I collagen fibril membranes (~0.1 pm/V) is roughly an order of magnitude lower than the local and macroscopic shear piezoresponse of D-periodic type I collagen fibrils within rat tail and bovine Achilles tendons (~1-2 pm/V) [13, 21, 24, 42]. The shear coefficient measured via PFM for D-periodic reconstituted collagen fibrils was 1.6 pm/V (calibrated data from ref. [24]). The reduction in the piezoelectric signal of the membranes therefore may be attributable to a lower degree of ordered molecular assembly, as evidenced by the lack of D-periodicity in the membranes, than is present in D-periodic collagen fibrils. The polar orientation of type I collagen fibrils is also retained in the *opaque* membrane, as seen in Fig. 4c as a 180° phase shift between opposing domains. The AFM height image of a 5×5 μm^2 area (Fig. 4d) compared with the

LPFM amplitude image in Fig. 4e reveals that each piezoelectric domain contains only ~1-3 fibrils. There are discontinuities in the collagen membrane, as highlighted by black arrows in Fig. 4d, which results in a low piezoelectric signal (shown in Fig. 4e). After neutralization, the topography of the *opaque* membrane appears altered (Fig. 5a). The fibrils have the same direction of alignment and do not exhibit the crimped structure visible in the *transparent* membrane. The measured width of the fibrils increased to 412 ± 51 nm, indicating a possible swelling of the fibrils, but this increase in fibril width is not statistically relevant. The LPFM amplitude image (Fig. 5b) reveals that the domain structure of the *opaque* membrane has also remained unchanged after neutralization. The averaged piezoresponse for 10 domains is 0.775 ± 0.058 a.u., which is only ~ 1.1 fold than that measured before neutralization, indicating that the change of pH does not affect the piezoelectric properties of the *opaque* membrane as significantly as it does for the *transparent* membrane. The crimped collagen structure obtained in the *transparent* membrane is formed by combining left-handed and right-handed helical-like arrays of fibrils into a double super-helix structure [34], whereas the *opaque* membrane has only a nematic orientation of helical-like arrays of fibrils. The presence of left-handed fibrils was also confirmed in rat tail tendon and ligament fibrillar crimps [47]. Thus, compared to the *opaque* membrane, the *transparent* membrane has an additional translational order in the direction perpendicular to the fibril alignment. Another significant difference between the two membranes is the larger fibrillar width present in the *opaque* membrane compared to that of the *transparent* membrane. The dependence of the piezoelectric response on the pH of collagen in the *transparent* membrane could therefore be attributable to a size or symmetry effect, the full elucidation of which would require further study beyond the scope of this work.

IV. Conclusion

Piezoresponse force microscopy experiments have been performed on collagen membranes having different structures at two different pH values in order to investigate the role of pH on surface structure and electromechanical properties. It was observed that there is a 1.35 fold increase in the lateral piezoresponse of the *transparent* membranes containing collagen nanofibrils when the pH is adjusted from acidic (pH = 2.5) to neutral (pH = 7) conditions. This increase in piezoresponse could be due to an increased activity of the polar bonds of collagen at neutral pH and further corresponds to a structural change in the membrane, namely the formation

of a crimp structure. In addition, shear piezoelectricity was observed in non D-periodic collagen fibrils. These results may force the re-evaluation of how piezoelectricity manifests in collagen. Piezoelectricity is generally attributed to the hexagonal packing of monomers within a collagen fibril. In the case of non D-periodic fibrils, this structure may not be accurate due to the incorrect lateral assembly of collagen molecules. Adjusting from acidic to physiological pH did not significantly change the lateral piezoresponse of the *opaque* membranes. The piezoelectric response has also been shown to be sensitive to whether collagen molecules are correctly assembled within a fibril. Interestingly, many diseases associated with collagen (e.g., *osteogenesis imperfecta*) are associated with the replacement of glycine in the collagen triple-helix with a larger amino acid [48]. This deforms the triple helix, affecting the structure and subsequent fibril assembly. In the case of collagen from femora in Brtl mice (model for *osteogenesis imperfecta*) [49], a larger variation in the periodicity was found in comparison to collagen from healthy mice. Thus, AFM and PFM may become a useful tool for distinguishing between, e.g., healthy and damaged or diseased tissue. The results shown here illustrate the pressing need for understanding exactly how piezoelectricity manifests itself in collagen and the implications this has on the biofunctionality of electromechanical coupling in not only bone, but all connective tissues.

Acknowledgements

This publication has emanated from research conducted with the financial support of Science Foundation Ireland under grant number SFI10/RFP/MTR2855 and was further facilitated by SFI13/CW/B2538. The authors gratefully acknowledge insightful discussions with A. Fertala, and COST action MP0904 for supporting training opportunities for early stage researchers. The authors also acknowledge the support of NANOREMEDIES, which is funded by the Programme for Research in Third Level Institutions, Cycle 5 and co-funded by the European Regional Development Fund. The AFM used for this work was funded by Science Foundation Ireland (SFI07/IN1/B931).

References

[1] Fukada E, Yasuda I. On the piezoelectricity of bone. J Phys Soc Jpn 1957;12:1158─1162.

[2] Fratzl P. Collagen: Structure and Mechanics. Springer Science+Business Media: New York; 2008.

[3] Fratzl P, Misof K, Zizak I, Rapp G, Amenitsch H, Bernstoff S. Fibrillar structure and mechanical properties of collagen. J Struct Bio 1998;122:119─122.

[4] Hay ED. Cellular interaction in extracellular matrix. Plenum Press; 1991.

[5] Akiyama SK, Nagata K, Yamada KM. Cell surface receptors for extracellular matrix components. Biochim Biophys Acta 1990;1031:91–110.

[6] Grinnell F. Fibroblast-collagen-matrix contraction: growth factor signaling and mechanical loading. Trends Cell Biol 2000;10:362–365.

[7] Grinnell F. Fibroblast biology in three-dimensional collagen matrices. Trends Cell Biol 2003;13:26426–26429.

[8] Gautieri A, Vesentini S, Redaelli A, Beuhler MJ. Hierarchical structure and nanomechanics of collagen microfibrils from the atomistic scale up. Nano Lett 2011;11:757–766.

[9] Gautieri A, Pate MI, Vesentini S, Redaelli A, Buehler MJ, 2012. Hydration and distance dependence of intermolecular shearing between collagen molecules in a model microfibril. J Biomech 2012;45:2079–2083.

[10] Liu Y, Wang Y, Chow M-J, Chen NQ, Ma F, Zhang Y, Li J. Glucose suppresses biological ferroelectricity in aortic elastin. Phys Rev Lett 2013;110:168101.

[11] Jiang F, Hörber H, Howard J, Müller DJ. Assembly of collagen into microribbons: effects of pH and electrolytes. J Struct Bio 2004;148:268–278.

[12] Ahn AC, Grodzinsky AJ. Relevance of collagen piezoelectricity to “Wolff’s Law”: a critical review. Med Eng Phys 2009;7:733–741.

[13] Fukada E, Yasuda I. Piezoelectric effects in collagen. Jpn J Appl Phys 1964;3: 117–121.

[14] Marino AA, Becker RO. Origin of the piezoelectric effect in bone. Calc Tiss Res 1971;8:177–180.

[15] Hulmes DJS, Miller A. Quasi-hexagonal molecular packing in collagen fibrils. Nature 1979;282:878–880.

[16] Kalinin SV, Rodriguez BJ, Jesse S, Karapetian E, Mirman B, Eliseev EA, Morozovska AN. Nanoscale electromechanics of ferroelectric and biological systems: A new dimension in scanning probe microscopy. Annu Rev Mater Res 2007;37: 189–238.

[17] Rodriguez BJ, Jesse S, Habelitz S, Proksch R, Kalinin SV. Intermittent contact mode piezoresponse force microscopy in a liquid environment. Nanotechnology 2009;20: 195701.

[18] Rodriguez BJ, Jesse S, Baddorf AP, Kalinin SV. High resolution electromechanical imaging of ferroelectric materials in a liquid environment by piezoresponse force microscopy. Phys Rev Lett 2006;96:237602.

[19] Balke N, Jesse S, Chi YH, Kalinin SV. High-frequency electromechanical imaging of ferroelectrics in a liquid environment. ACS Nano 2012;6:5559–5565.

[20] Halperin C, Mutchnik S, Agronin A, Molotskii M, Urenski P, Salai M, Rosenman G. Piezoelectric Effect in Human Bones Studied in Nanometer Scale. Nano Letters 2004;4:1253–1256.

[21] Minary-Jolandan M, Yu MF. Nanoscale characterization of isolated individual type I collagen fibrils: polarization and piezoelectricity. Nanotechnology 2009;20:085706.

[22] Minary-Jolandan M, Yu MF. Uncovering nanoscale electromechanical heterogeneity in the subfibrillar structure of collagen fibrils responsible for the piezoelectricity of bone. ACS Nano 2009;3:1859–1863.

[23] Hutmacher DW. Scaffold design and fabrication technologies for engineering tissues: state of the art and future perspectives. J Biomater Sci Polym E 2001;12:107–24.

[24] Denning D, Abu-Rub MT, Zeugolis DI, Habelitz S, Pandit A, Fertala A, Rodriguez BJ. Electromechanical properties of dried tendon and isoelectrically focused collagen hydrogels. Acta Biomater 2012;8:3073–3079.

[25] Liu Y, Zhang Y, Chow MJ, Chen QN, Li J. Biological ferroelectricity uncovered in aortic walls by piezoresponse force microscopy. Phys Rev Lett 2012;108:078103.

[26] Heredia A, Meunier V, Bdikin IK, Gracio J, Balke N, Jesse S, Tselev A, Agarwal PK, Sumpter BG, Kalinin SV, Kholkin AL. Nanoscale ferroelectricity in crystalline γ-glycine. Adv Funct Mater 2012;22:2996–3003.

[27] Lee BY, Zhang J, Zueger C, Chung WJ, Yoo SO, Wang E, Meyer J, Ramesh R, Lee SW. Virus-based piezoelectric energy generation. Nat Nanotech 2012;7:351–326.

[28] Rodriguez BJ, Kalinin SV, Shin J, Jesse S, Grichko V, Thundat T, Baddorf AP, Gruverman A. Electromechanical imaging of biomaterials by scanning probe microscopy. J Struc Bio 2006;153:151–159.

[29] Paukshto M, McMurtry D, Bobrov Yu, Sabelman E. Oriented collagen-based materials, films and methods of making same. PCT/US2008/060919.

[30] Paukshto M, Fuller G, Mikhailov A, Remisov S. Optics of sheared liquid crystal polarizer based on aqueous dispersion of dichroic dye nano-aggregates. J Soc Inf Display 2005;13:765–772.

[31] Ukai Y Ohyama T, Fennell L, Kato Y, Paukshto M, Smith P, Yamashita O, Nakanishi S. Current Status and Future Prospect of In-Cell Polarizer Technology. J Soc Inf Displya. 2004;13:17–24.

[32] Fennel L, Lazarev P, Ohmura S, and Paukshto M. Thin Crystal Film Polarizers. Asia Display/IDW'01. Proceedings of The 21st International Display Research Conference in conjunction with The 8th International Display Workshops. Nagoya. Japan. 2001;601–603.

[33] Giraud-Guille MM, Mosser G, Belamie E. Liquid crystallinity in collagen systems in vitro and in vivo, Current Opinion in Colloid & Interface Science 2008;13:303–313.

[34] McMurtry D, Paukshto M, Bobrov Yu. A liquid film applicator assembly and rectilinear shearing system incorporating the same. PCT/US2007/02238.

[35] Peter F, Reichenberg B, Rüdiger A, Waser R, Szot K. Sample-tip interaction of piezoelectric force microscopy in ferroelectric nanostructures. IEEE Trans Ultrason Ferroelectr Freq Control 2006;53:2253–2260.

[36] Komai Y, Ushiki T, The three-dimensional organization of collagen fibrils in the human cornea and sclera. Invest Opthalmol Vis Sci 1991;32:2244–2258.

[37] Holmes DF, Gilpin CJ, Baldock C, Ziese U, Koster AJ, Kadler KE. Corneal collagen fibril structure in three dimensions: structural insights into fibril assembly, mechanical properties and tissue organization. PNAS 2001;98:7307–7312.

[38] Muthusubramaniam L, Peng L, Zaitseva T, Paukshto M, Martin GR, Desai TA. Collagen fibril diameter and alignment promote the quiescent keratocyte phenotype. J Biomed Mater Res Part A 2012:100A:613–621.

[39] Scott JE, Orford CR, Hughes EW. Proteoglycan-collagen arrangements in developing rat tail tendon. An electron microscopical and biochemical investigation.

Biochem J 1981;195:573–581.
[40] Denning D, Aliat S, Habelitz S, Fertala A, Rodriguez BJ. Visualizing molecular polar order in tissues via electromechanical coupling. J Struct Bio 2012;180:409–419.
[41] Hong S, Woo J, Shin H, Jeon JU, Pak YE. Principle of ferroelectric domain imaging using atomic force microscope. J Appl Phys 2001;89:1377.
[42] Harnagea C, Vallières M, Pfeffer CP, Wu D, Olsen BR, Pignolet A, Lègarè F, Gruverman A. Two-dimensional nanoscale structural and functional imaging in individual collagen type I fibrils. Biophys J 2010;12:3070–3077.
[43] Freed AD, Doehring TC. Elastic model for crimped collagen fibrils. J Biomech Eng 2005;27:587–593.
[44] Suzuki Y, Someki I, Adachi E, Irue S, Hattori S. Interaction of collagen molecules from the aspect of fibril formation: acid-soluble, alkali-treated, and MMP1-digested fragments of type I collagen. J Biochem 1999;126:54–67.
[45] Netto TG, Zimmerman RL. Effect of water on piezoelectricity in bone and collagen. Biophys J 1975:15;573–576.
[46] Petsko GA, Ringe D. Protein structure and function. New Science Press Ltd. U.K. 2003.
[47] Franchi M, Ottani V, Stagni R, Ruggeri A. Tendon and ligament fibrillar crimps give rise to left-handed helices of collagen fibrils in both planar and helical crimps. J Anat 2010; 216: 301–309.
[48] Kuivaniemi H, Tromp G, Prockop DJ. Mutations in collagen genes: causes of rare and some common diseases in humans. FASEB J 1991;7:2052–2060.
[49] Wallace JM, Orr BG, Marini JC, Holl MM. Nanoscale morphology of type I collagen is altered in the Brtl mouse model of osteogenesis imperfecta. J Struct Biol 2011;1:146–152.

Figure Captions

Figure 1. AFM images of *transparent* and *opaque* collagen membranes. (a) AFM height image of a *transparent* collagen membrane (z-scale = 90 nm; scale bar = 500 nm). Inset displays the AFM amplitude image of the same area as shown in (a) (z-scale = 30 nm). (b) AFM height image (z-scale = 40 nm; scale bar = 200 nm). (c) AFM amplitude image, where black arrows highlight non-periodic structure in the fibrils (z-scale = 12 nm). (d) AFM height image of the *opaque* membrane (z-scale = 550 nm; scale bar = 5 μm). Inset shows AFM amplitude image of same area as (d) (z-scale = 110 nm). (e) AFM height image of the *opaque* membrane (z-scale = 400 nm; scale bar = 2 μm). (f) AFM amplitude image (z-scale 50 nm).

Figure 2. LPFM images of the *transparent* collagen membrane before the neutralization process. (a) AFM contact mode height image (z-scale = 170 nm; scale bar = 2 μm). White arrow indicates fibrillar alignment. (b) LPFM amplitude image of area in (a). (c) LPFM phase image revealing polarity of each domain. (d) AFM height image of *transparent* collagen membrane (z-scale = 70 nm; scale bar = 1 μm). (e) LPFM amplitude image of area in (a). (f) LPFM phase image. White arrows in (d-f) highlight individual fibril showing evidence of polarity reversal due to the change in orientation with respect to the cantilever axis. The yellow arrow in (d) indicates the scanning direction of cantilever.

Figure 3. LPFM images of *transparent* collagen membrane after the neutralization process. (a) AFM height image of a *transparent* collagen membrane after neutralization (z-scale = 80 nm; scale bar = 2 μm). (b) LPFM amplitude image illustrating a similar domain structure as seen before the process. (c) LPFM phase image showing retention of the polarity of collagen domains. (e) AFM height image (z-scale = 40 nm; scale bar = 1 μm). Dashed white line highlights the crimp structure. (e) LPFM amplitude image of area shown in (d) and corresponding (f) LPFM phase image.

Figure 4. LPFM images of non D-periodic *opaque* collagen membrane before the neutralization process. (a) AFM height image displaying collagen fibrils (scale bar = 2 μm). (b) LPFM amplitude image. (c) LPFM phase image. (d) AFM height image (scale bar = 1 μm). (e) LPFM

amplitude image of area shown in (d). Black arrows in (d) and (e) emphasize reduced piezoresponse signal from discontinuities in the collagen matrix. (f) LPFM phase image displaying polarity of domains. The z-scale for (a) and (d) is 700 nm.

Figure 5. LPFM images of *opaque* collagen membrane after the neutralization process. (a) AFM height image displaying non D-periodic collagen fibrils (z-scale = 560 nm; scale bar = 2 μm). (b) LPFM amplitude image of same area in (a) displaying retention of piezoelectric domains as seen before neutralization. (c) LPFM phase image mapping the polarity of domains in (b). (d) AFM height image (z-scale = 200 nm; scale bar = 1 μm). (e) LPFM amplitude image of area shown in (d) and corresponding (f) LPFM phase image displaying polarity of domains.

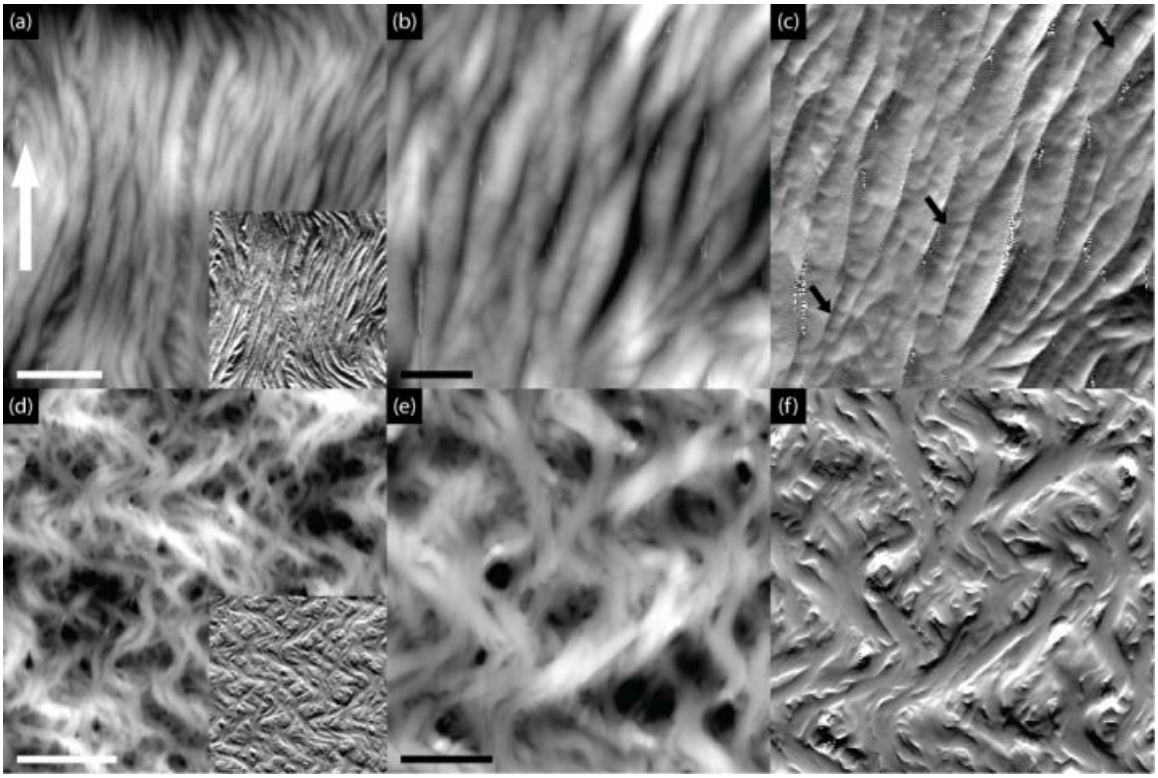

Figure 1

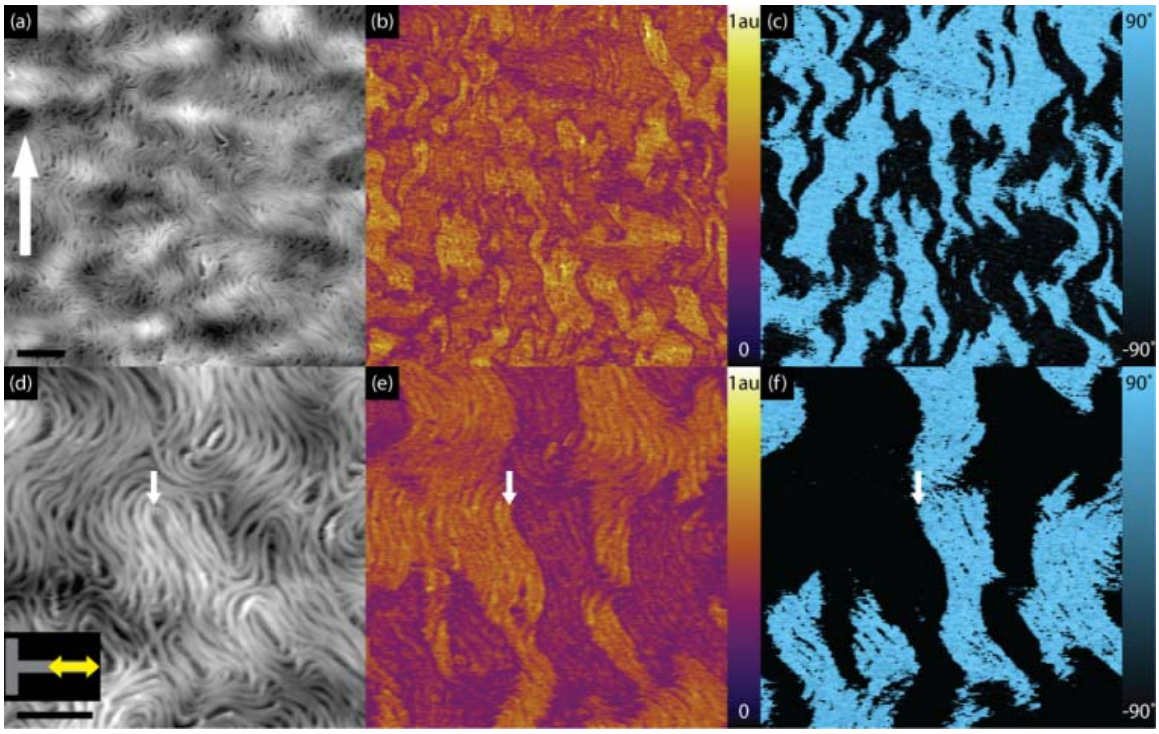

Figure 2

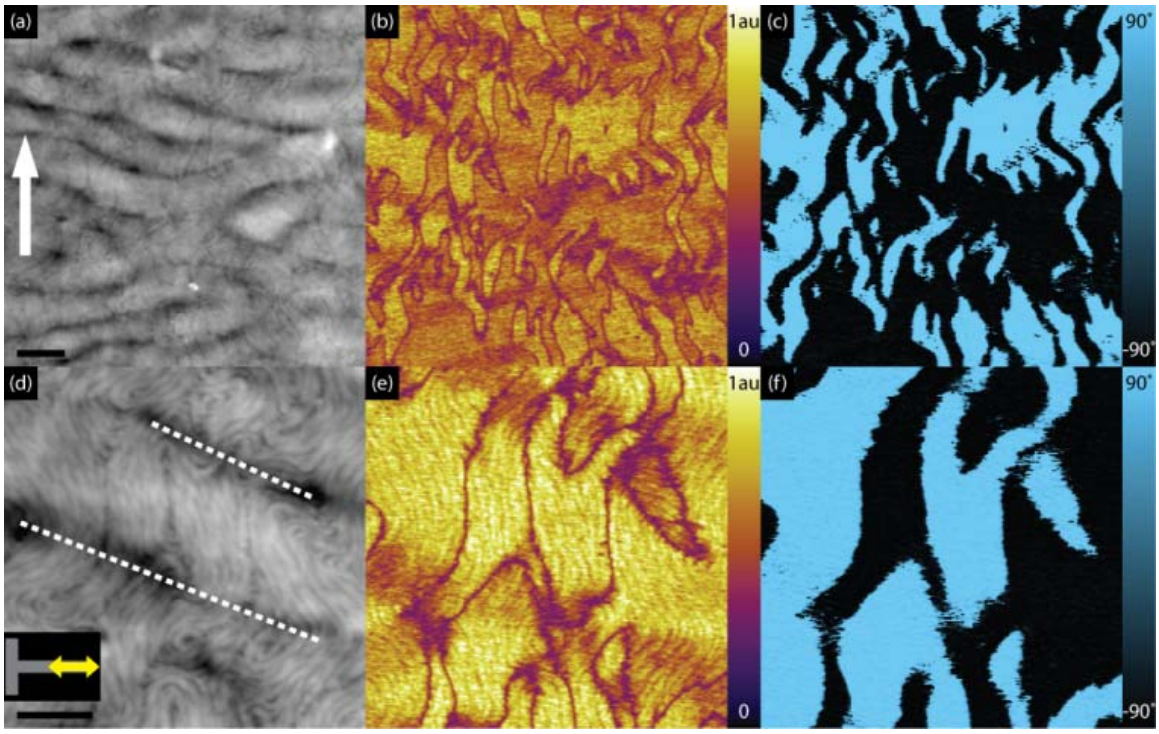

Figure 3

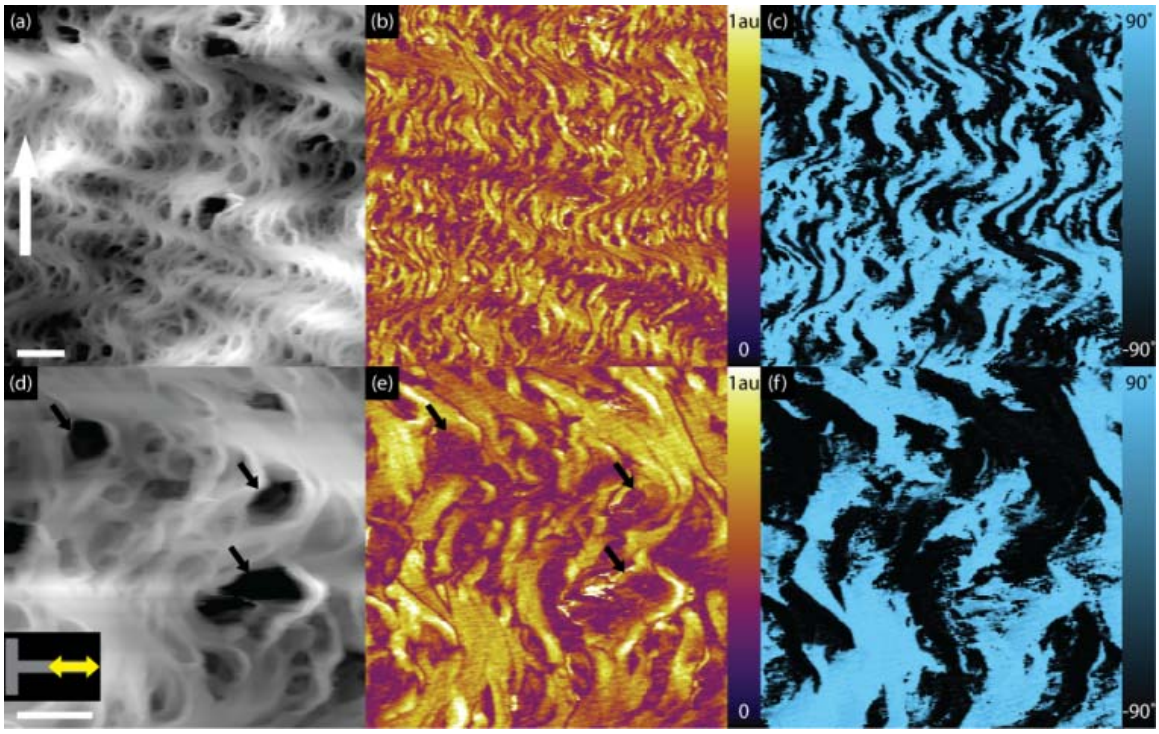

Figure 4

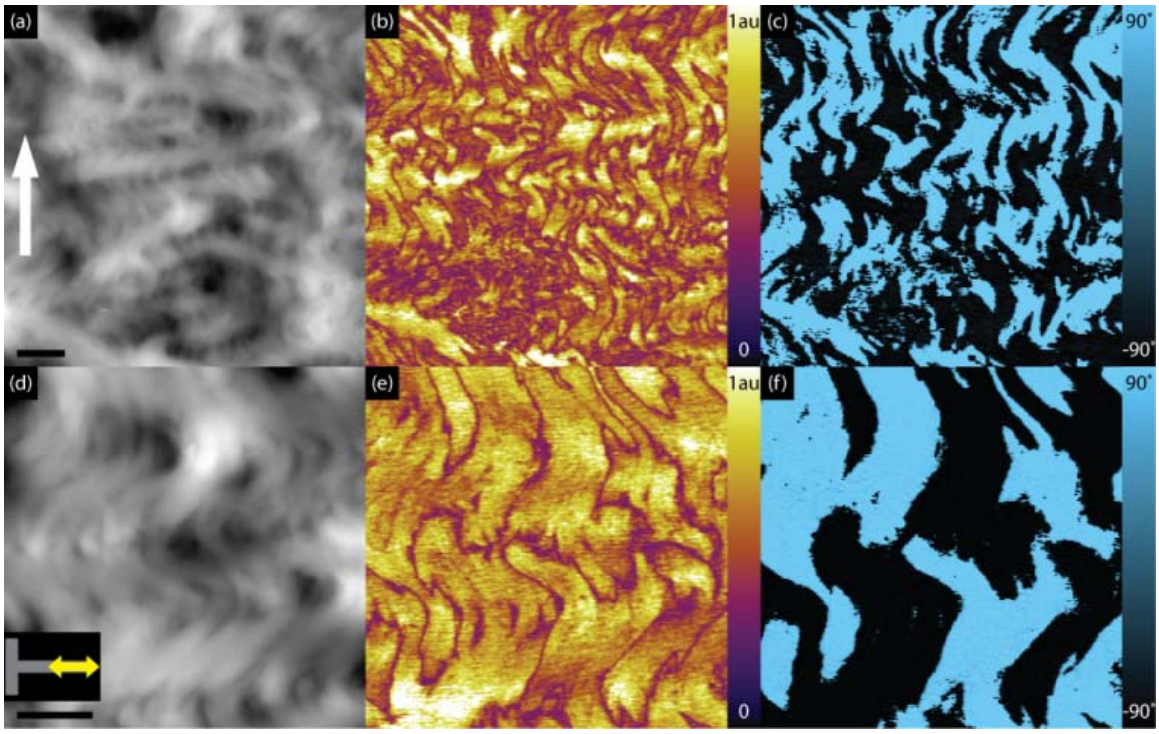

Figure 5